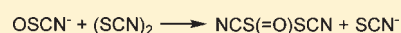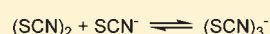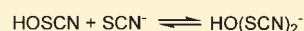# Mechanism of Decomposition of the Human Defense Factor Hypothiocyanite Near Physiological pH

József Kalmár, Kelemu L. Woldegiorgis, Bernadett Biri, and Michael T. Ashby*

Department of Chemistry and Biochemistry, University of Oklahoma, Norman, Oklahoma 73019, United States

Ⓢ *Supporting Information*

ABSTRACT: Relatively little is known about the reaction chemistry of the human defense factor hypothiocyanite ($OSCN^-$) and its conjugate acid hypothiocyanous acid (HOSCN), in part because of their instability in aqueous solutions. Herein we report that HOSCN/$OSCN^-$ can engage in a cascade of pH- and concentration-dependent comproportionation, disproportionation, and hydrolysis reactions that control its stability in water. On the basis of reaction kinetic, spectroscopic, and chromatographic methods, a detailed mechanism is proposed for the decomposition of HOSCN/$OSCN^-$ in the range of pH 4–7 to eventually give simple inorganic anions including CN^-, OCN^-, SCN^-, SO_3^{2-}, and SO_4^{2-}. Thiocyanogen ($(SCN)_2$) is proposed to be a key intermediate in the hydrolysis; and the facile reaction of $(SCN)_2$ with $OSCN^-$ to give NCS(=O)SCN, a previously unknown reactive sulfur species, has been independently investigated. The mechanism of the aqueous decomposition of $(SCN)_2$ around pH 4 is also reported. The resulting mechanistic models for the decomposition of HOSCN and $(SCN)_2$ address previous empirical observations, including the facts that the presence of SCN^- and/or $(SCN)_2$ decreases the stability of HOSCN/$OSCN^-$, that radioisotopic labeling provided evidence that under physiological conditions decomposing $OSCN^-$ is not in equilibrium with $(SCN)_2$ and SCN^-, and that the hydrolysis of $(SCN)_2$ near neutral pH does not produce $OSCN^-$. Accordingly, we demonstrate that, during the human peroxidase-catalyzed oxidation of SCN^-, $(SCN)_2$ cannot be the precursor of the $OSCN^-$ that is produced.

$$HOSCN \rightleftharpoons OSCN^- + H^+$$
$$HOSCN + SCN^- \rightleftharpoons HO(SCN)_2^-$$
$$HO(SCN)_2^- \rightleftharpoons (SCN)_2 + OH^-$$
$$HO(SCN)_2^- + H^+ \rightleftharpoons (SCN)_2 + H_2O$$
$$(SCN)_2 + SCN^- \rightleftharpoons (SCN)_3^-$$
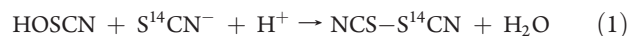$$OSCN^- + (SCN)_2 \longrightarrow NCS(=O)SCN + SCN^-$$

INTRODUCTION

There are approximately 200 references in the primary literature that explicitly mention HOSCN and/or $OSCN^-$.[1,2] The publications are roughly equally distributed in the dental, food, medical, and chemical literature. A very large number of additional publications certainly concern $OSCN^-$; however, they do not explicitly mention the compound. For example, nearly 6000 journal articles involve the enzyme lactoperoxidase, for which SCN^- is known to be the substrate in vivo, and $OSCN^-$ is the only known product.[3,4] Interestingly, many of the publications in dental[1,5,6] and dairy[7-11] literature predate most of the chemical studies. Indeed, much of the current interest in $OSCN^-$ is derived from its relevance in food science and medicine.[12,13] There appears to be a regrettable lack of communication between these disciplines; consequently, many inconsistencies exist in literature, particularly concerning the chemistry. In addition, the primary conclusions of many of these studies have been rendered suspect due to relatively recent advances in our understanding of the chemistry which suggest that $OSCN^-$ should not exist under the conditions employed in some of the studies. Finally, while it is generally assumed that $OSCN^-$ is the only biologically active species produced from the oxidation of SCN^- in vivo, it is clear that many potentially active species must be formed during the redox/hydrolysis cascade of $OSCN^-$ that produces the eventual products CN^-, OCN^-, SO_3^{2-}, and SO_4^{2-}.[14,15]

Until now, there have been no methodical investigations of the kinetics and mechanisms of the decomposition of $OSCN^-$ near physiologically relevant neutral pH conditions. However, anecdotal reports indicate that the decomposition of $OSCN^-$ is faster at low pH and with high concentrations of SCN^-. Considering the observation that $(SCN)_2$ does not yield $OSCN^-$ when it is hydrolyzed at neutral pH,[15-18] one might conclude that the comproportionation of HOSCN and SCN^- to give $(SCN)_2$ is involved in the decomposition mechanism of $OSCN^-$ near neutral pH. However, isotopic exchange of the C atoms of $OSCN^-$ and SCN^- is not observed near neutral pH, as might be expected for a reversible comproportionation:[19]

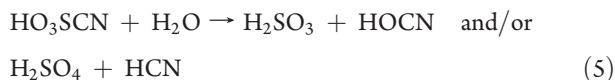$$HOSCN + S^{14}CN^- + H^+ \rightarrow NCS - S^{14}CN + H_2O \quad (1)$$

$$NCS - S^{14}CN + H_2O \rightarrow HOS^{14}CN + SCN^- + H^+ \quad (2)$$

It is furthermore noteworthy that $(SCN)_2$ accelerates the decomposition of $OSCN^-$ (i.e., $OSCN^-$ and $(SCN)_2$ react even at neutral pH before the latter species decomposes; vide infra). When HOSCN is reacted with $^{35}SCN^-$, the SO_4^{2-} that is obtained does not contain the label. While the ^{14}C and ^{35}S tracer studies do not preclude the involvement of NCSCN, O_2SCN^-, O_3SCN^-, and other possible intermediates, they suggest that the reversible equilibrium between $OSCN^-$ and $(SCN)_2$ in the presence of SCN^- (eqs 1 and 2) is not involved in the decomposition mechanism. The eventual decomposition products of $OSCN^-$ are CN^-, OCN^-, SO_3^{2-}, and SO_4^{2-}, depending on the specific reaction conditions. These products may be accounted for

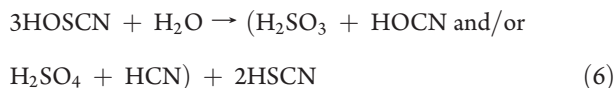by the following atom/electron balance (eqs 3−5, which does not necessarily reflect the intimate mechanism or the intermediates that are involved):

$$2HOSCN \rightarrow HO_2SCN + HSCN \qquad (3)$$

$$HO_2SCN + HOSCN \rightarrow HO_3SCN + HSCN \qquad (4)$$

$$HO_3SCN + H_2O \rightarrow H_2SO_3 + HOCN \quad and/or$$

$$H_2SO_4 + HCN \qquad (5)$$

which yield the net reaction of eq 6:

$$3HOSCN + H_2O \rightarrow (H_2SO_3 + HOCN \; and/or$$

$$H_2SO_4 + HCN) + 2HSCN \qquad (6)$$

It has been previously suggested that the mechanism involves dismutation of HOSCN (eq 3) because second-order kinetics have been observed under pH conditions where $OSCN^-$ + HOSCN predominate.[18,20] However, others have reported first-order kinetics for the decomposition of $OSCN^-$ (and under specific conditions we have observed first-order kinetics as well; vide infra).[19] The mechanism of eqs 3−5 has been proposed to produce H_2SO_4 + HCN,[20] but CN^- is not produced quantitatively, presumably because it reacts with HOSCN to produce NCSCN, which subsequently hydrolyzes to produce a 1:1 mixture of SCN^- and OCN^-.[21] Importantly, although there is no experimental evidence for the intermediates that are involved in the decomposition of $OSCN^-$, cyanosulfite, O_2SCN^-,[22,23] and cyanosulfate, O_3SCN^-,[24] have been observed in nonaqueous media (but not in water). However, many other potential intermediates are possible, including the unknown anhydride (cf. thiosulfinate esters, the anhydrides of sulfenic acids):

$$2HOSCN \rightarrow NCS(=O)SCN + H_2O \qquad (7)$$

In the present study we investigate the decomposition of HOSCN and $(SCN)_2$ in detail around pH 4.0 in acetate buffer, as well as the decomposition of $OSCN^-$ around pH 7.0 in phosphate buffer, and show that the observed mechanisms are relevant to the stability of $OSCN^-$ at physiological pH. As SCN^- is considered to be a pseudo-halide in several aspects of reactivity,[25−27] we base some of our considerations on analogous hydrolysis chemistry of halogens.[28−30]

■ RESULTS

Decomposition of HOSCN/$OSCN^-$ around pH 4. The kinetics of the reaction were studied in the range from pH 4.3 to pH 6.0. Because the pK_a of HOSCN is 4.85,[31] a mixture of HOSCN and $OSCN^-$ was present. The decomposition of HOSCN/$OSCN^-$ was monitored photometrically at multiple wavelengths from 290 to 705 nm; two spectral features were observed: at 306 (shoulder) and 376 nm (maximum) (Figure S2 of the Supporting Information). According to the singular value decomposition (SVD) analysis of multiwavelength data (SpecFit32), the reaction follows strict pseudo-first-order kinetics when SCN^- is in large excess over HOSCN/$OSCN^-$. Second-order kinetics were never observed during the experiments.[14,15] The half-life of the decomposition of HOSCN/$OSCN^-$ is ~0.5 s, depending on the actual conditions (Figure S2). For constant $[SCN^-]$ and $[H^+]$, principal component analysis (PCA) of the collected time-resolved spectra showed the overdominating variance of the first component
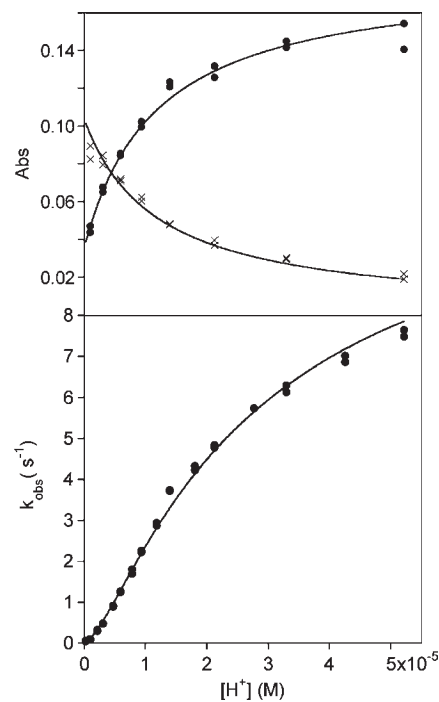
Figure 1. pH dependence of the initial absorbance (A_0, top) and the observed pseudo-first-order rate constants (k_{obs}, bottom) of the decomposition of HOSCN + $OSCN^-$ in the range from pH 4.37 to pH 5.66. Markers: measured data (top: dots, 306 nm; crosses, 376 nm). Lines: results of global data fit. $[HOSCN]_{T,0}$ = 3.5 mM, $[SCN^-]$ = 0.25 M, $[HOAc]$ + $[OAc^-]$ = 0.50 M, μ = 1.0 M, 25.0 °C.

(i.e., no absorbing intermediate is present at detectable quantities during the decomposition over wide ranges of $[SCN^-]$ and pH). The measured pseudo-first-order rate constants (k_{obs}) were found to be invariable to the buffer concentration and to the initial analytical HOSCN concentration ($[HOSCN]_{T,0}$ = $[HOSCN]_0$ + $[OSCN^-]_0$). The values of k_{obs} are directly proportional to $[SCN^-]$ over 1 order of magnitude change in $[SCN^-]$, with a negligible ordinate intercept (Figure S3 of the Supporting Information). The $[H^+]$ dependency of the reaction is complex. At constant $[SCN^-]$ the initial spectrum of the reactant solution recorded 0.75 ms after the jump to the desired pH (second mixing) is pH-dependent as seen in Figure 1. The series of the initial spectra recorded at different pH can be successfully analyzed by taking into account only the protolytic equilibrium between HOSCN (A_{max} at 306 nm) and $OSCN^-$ (A_{max} at 376 nm) (Figure S4 of the Supporting Information). Figure 1 illustrates that the values of k_{obs} increase with $[H^+]$. The k_{obs} vs $[H^+]$ curve is sigmoidal, and it can be fit to the following function:

$$k_{obs} = \frac{\xi'_1[H^+]^2}{\xi_2 + \xi_3[H^+] + [H^+]^2} \qquad (8)$$

where ξ'_1, ξ_2, and ξ_3 are pH-independent constants. If we take into account that k_{obs} is directly proportional to $[SCN^-]$, the following rate law is deduced:

$$v = \frac{\xi_1[H^+]^2[SCN^-]}{\xi_2 + \xi_3[H^+] + [H^+]^2}[HOSCN]_T \qquad (9)$$

where ξ_1, ξ_2, and ξ_3 are constants (the values of ξ are given in Table S2 of the Supporting Information) and $[HOSCN]_T$ is the

Table 1. Relative Concentrations of Decomposition Products As Determined by Ion Chromatography[a]

	relative concentration, %					
	OCN^-	CN^-	SO_3^{2-}	SO_4^{2-}	SCN^-	HOSCN + CN^- pathway, %
HOSCN/OSCN$^-$ (pH = 4.33)	11 ± 2 (17)	8 ± 2 (11)	2 ± 1 (3)	20 ± 6 (25)	69 ± 6 (71)	14
OSCN$^-$ (pH = 6.82)	53 ± 8 (27)	0 (0)	5 ± 2 (8)	17 ± 4 (19)	55 ± 8 (73)	19
(SCN)$_2$ (pH = 3.89)	12 ± 2 (12)	23 ± 5 (19)	4 ± 1 (4)	22 ± 2 (27)	159 ± 7 (169)	8
(SCN)$_2$ (pH = 6.90)	59 ± 6 (28)	0 (0)	7 ± 2 (10)	18 ± 1 (18)	144 ± 13 (172)	17

[a] Parentheses: calculated values based on the proposed stoichiometry of the reactions (Schemes 1 and 2) and on the indicated contribution to the total consumption of the reactants of the HOSCN + CN$^-$ pathway (Scheme 3, R14).

time-dependent analytical concentration of HOSCN + OSCN$^-$ in the reaction mixture.

To study the reversibility of the decomposition of HOSCN/OSCN$^-$, triple-mixing stopped-flow experiments with in situ UV−vis detection were performed. When aging times of $\tau_2 < 6t_{1/2}$ were employed using an acidic quench to produce (SCN)$_2$ and a basic quench to produce OSCN$^-$,[14,15,32] the reactions were complete within the mixing time. The amount of (SCN)$_2$ or OSCN$^-$ formed was quantitatively the same as the remaining amount of HOSCN/OSCN$^-$ that was expected at the time of quenching its decomposition mixture (Figure S5 of the Supporting Information). At aging times $\tau_2 > 7t_{1/2}$, no spectral change was observed after quenching.

Electrospray ionization mass spectrometry (ESI-MS) experiments provided evidence for the formation of CN$^-$, OCN$^-$, SO$_4^{2-}$, and traces of SO$_3^{2-}$ during the decomposition of HOSCN/OSCN$^-$ around pH 4. No intermediates, only the end products and OSCN$^-$ from the basic quench, were identified in the triple-mixing quench-flow/ESI-MS experiments. The amount of products relative to [HOSCN]$_{T,0}$ are given in Table 1. The measured amounts of products were invariable to the presence of excess SCN$^-$ during the decomposition.

Decomposition of HOSCN/OSCN$^-$ around pH 7. The kinetics of the decomposition of OSCN$^-$ were studied in the pH range of 6.1−7.2. The reaction is strictly pseudo-first-order when SCN$^-$ is in a large excess over OSCN$^-$, with a half-life of ∼20 s. PCA of time-resolved photometric data revealed only one detectable absorbing species (A_{max} at 376 nm) during the reaction. The value of k_{obs} was independent of the initial OSCN$^-$ concentration and independent from the buffer concentration. k_{obs} is proportional to [SCN$^-$] with a nonzero intercept (Figure S6 of the Supporting Information):

$$k_{obs} = \xi_4[SCN^-] + \xi_5 \tag{10}$$

where ξ_4 and ξ_5 are [SCN$^-$]-independent constants. The initial spectrum of the reactant solution recorded 0.75 ms after pH jump is independent of [H$^+$], although k_{obs} is proportional to [H$^+$] with a nonzero ordinate intercept (Figure S6):

$$k_{obs} = \xi_6[H^+] + \xi_7 \tag{11}$$

where ξ_6 and ξ_7 are pH-independent constants. From the fitted lines (e.g., Figures S6 and Table S2), a simple calculation leads to the following: $\xi_4/[H^+] = \xi_6/[SCN^-]$ and $\xi_5 = \xi_7$. Thus, the rate law for the decomposition of OSCN$^-$ at pH 7 is

$$v = (\xi_8[H^+][SCN^-] + \xi_9)[HOSCN]_T \tag{12}$$

where ξ_8 and ξ_9 are constants, $\xi_8 = \xi_4/[H^+] = \xi_6/[SCN^-]$ $\xi_9 = \xi_5 = \xi_7$ (Table S2), and [HOSCN]$_T$ is the time-dependent
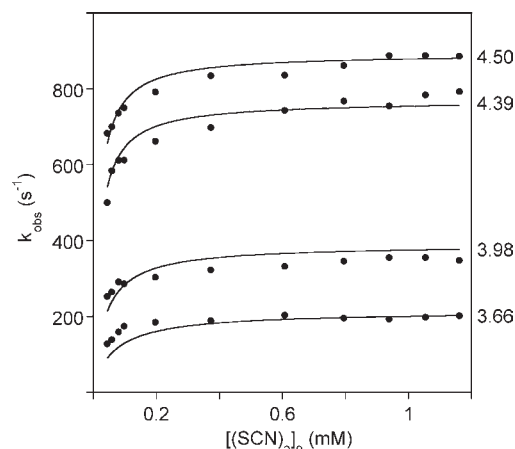
**Figure 2.** Effect of $[(SCN)_2]_{T,0}$ (the initial concentration of (SCN)$_2$ + (SCN)$_3^-$ + HO(SCN)$_2^-$; see Discussion for details) on the observed pseudo-first-order rate constants for the hydrolysis of (SCN)$_2$ in the range from pH 3.66 to pH 4.50 (indicated to the right from the plots): (dots) measured data; (lines) results of global data fit. The kinetics of the reaction deviates from pseudo-first-order at low $[(SCN)_2]_{T,0}$. [SCN$^-$] = 0.25 M, [HOAc] + [OAc$^-$] = 0.50 M, μ = 1.0 M, and 25.0 °C.

analytical concentration of HOSCN + OSCN$^-$ in the reaction mixture. Acidic and basic triple-mixing quench studies were performed, and the amount of (SCN)$_2$ or OSCN$^-$ formed was the same as the remaining amount of OSCN$^-$ that was expected at the time of quenching.

The ions OCN$^-$, SO$_4^{2-}$, and SO$_3^{2-}$ were identified in the ESI-MS spectra of the sample produced during the decomposition of OSCN$^-$ around pH 7. Evidence was also found for the formation of elementary sulfur as HS$_3^+$ at m/z = 96.9228 was present in the +ESI-MS spectrum of the product solution. According to the ion chromatography (IC) measurements, the proportions of the products are significantly different from that observed in acetate buffer as seen in Table 1. The measured product distribution around pH = 7 was the same regardless of whether OSCN$^-$ was generated from (SCN)$_2$ or by the LPO/SCN$^-$/H$_2$O$_2$ system. No effect of an initial SCN$^-$ excess was observed on the product distribution.

Decomposition of (SCN)$_2$ around pH 4. Kinetic studies were performed in the range of pH 3.8−4.7. Since both (SCN)$_2$ and SCN$^-$ were present in the solutions, (SCN)$_3^-$ is formed in equilibrium.[14] The latter equilibration is established in the mixing time over the entire range of pH.[14,15,33] The majority of the kinetic experiments were followed at 300 nm, which is the absorbance maximum of (SCN)$_3^-$.[14,15,33] On the basis of the UV−vis and MS spectra (vide infra) of the resulting solutions,
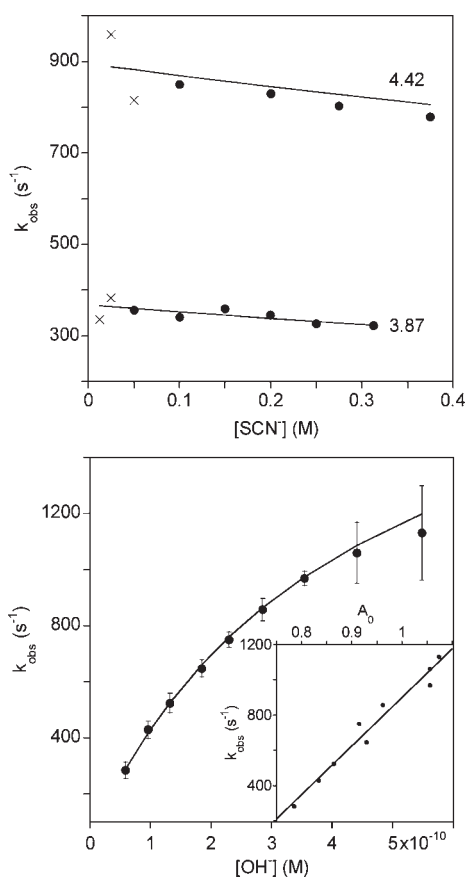
Figure 3. pH and $[SCN^-]$ dependence of k_{obs} of the decomposition of $(SCN)_2$ in the range from pH 3.77 to pH 4.74. Top, $[SCN^-]$ dependence: the initial concentration of $(SCN)_2$ varied with $[SCN^-]$ at pH 3.87 and pH 4.42 (see explanation in text); (dots) measured data at high $[(SCN)_2]_{T,0}$ from 1.0 to 0.4 mM; (crosses) measured data at lower $[(SCN)_2]_{T,0}$ from 0.4 to 0.1 mM; (line) result of global data fit. $[HOAc] + [OAc^-] = 0.50$ M, $\mu = 1.0$ M, and $T = 25.0$ °C. Bottom, pH dependence: (dots) measured data; (line) result of global fit; (inset) k_{obs} proportional to the calculated initial absorbance at 300 nm (A_0^{CALC}). $[(SCN)_2]_{T,0} = 1.0$ mM, $[SCN^-] = 0.25$ M, $[HOAc] + [OAc^-] = 0.50$ M, $\mu = 1.0$ M, and 25.0 °C.

the product of the hydrolysis of the $(SCN)_2/(SCN)_3^-$ mixture is not $HOSCN/OSCN^-$. The reaction follows first-order kinetics in the presence of a large excess of SCN^- with a half-life of 2−4 ms, depending on the actual conditions (Figure S7 of the Supporting Information). The kinetic curves recorded at high $[(SCN)_2]_{T,0}$ (vide infra) cannot be fit with second-order functions, and the least-squares residuals are the same for single-exponential and biexponential fits.

As expected, k_{obs} is generally independent of $[(SCN)_2]_{T,0}$. However, for $[(SCN)_2]_{T,0}$ lower than ∼200−300 μM, k_{obs} decreases with decreasing $[(SCN)_2]_{T,0}$ (Figure 2). The photometric data were exceptionally low quality under these conditions because the measured absolute change was only about 0.03 absorbance unit, which is comparable to the level of the noise in the first few milliseconds of the measurements as a consequence of the shock of the stopped-flow mixing cycle. Nonetheless, least-squares fit of the kinetic curves gives better results with first-order than with second-order kinetic functions. The $[(SCN)_2]_{T,0}$ was established by two different means: (1) by changing the concentration of HOCl in the first mixing cycle and (2) at constant

$[HOCl]_0$ by changing the aging time before the second mixing cycle (τ_1), thus allowing the in situ-generated $(SCN)_2$ to decompose at pH 0.7 to various extents. The independent sets of experiments gave identical results (Figure S8 of the Supporting Information). The kinetic curves recorded at low $[(SCN)_2]_{T,0}$ match the end of the kinetic curves recorded at high $[(SCN)_2]_{T,0}$ under the same conditions (Figure S8). However, when starting at high $[(SCN)_2]_{T,0}$ the theoretical error of treating the whole course of decomposition as a pseudo-first-order process and fitting k_{obs} accordingly is negligible, as only the last 5−10% of the data deviates significantly from the single-exponential function which fits the majority of the curve.

The following results were obtained at high $[(SCN)_2]_{T,0}$ unless stated otherwise. PCA of time-resolved multiwavelength photometric data revealed that only one absorbing species (A_{max} at 300 nm) is detectable during the reaction from 290 to 705 nm at a given $[SCN^-]$ and $[H^+]$. The pseudo-first-order kinetic curves measured at 300 nm were extrapolated using single-exponential functions to −0.6 ms (time correction; see details in Supporting Information). The calculated zero-time absorbance at 300 nm (A_0^{CALC}) increases sigmoidally with $[SCN^-]$ at constant $[H^+]$ (Figure S9 of the Supporting Information). Two effects are evident in the A_0^{CALC} vs $[SCN^-]$ curve: (1) shifting of the $(SCN)_2/(SCN)_3^-$ rapid equilibrium and (2) the rate of decomposition of the in situ-generated $(SCN)_2$ at pH = 0.7 in the first mixing cycle shows an inverse second-order dependence on $[SCN^-]$.[14,15] Thus, at lower $[SCN^-]$, the $[(SCN)_2]_{T,0}$ is less after the τ_1 first aging-time (Figure S9; see details in the Supporting Information). Data recorded at high and low $[(SCN)_2]_{T,0}$ showed consistency; k_{obs} is inversely dependent on $[SCN^-]$ (as seen in Figure 3):

$$k_{obs} = \frac{\xi_{10}}{1 + \xi_{11}[SCN^-]} \qquad (13)$$

where both ξ_{10} and ξ_{11} are $[SCN^-]$-independent constants. ξ_{10} increases with increasing pH, and ξ_{11} slightly decreases with increasing pH (Table S2). At constant $[SCN^-]$, independent from $[(SCN)_2]_{T,0}$, A_0^{CALC} increases to saturation with increasing pH (Figure S10 of the Supporting Information). The initial spectrum of the reaction mixture recorded at different pH values ($t = 1.5$ ms) displays only one peak at 300 nm; thus, the fast equilibrium which yields $HOSCN/OSCN^-$ is not relevant under the conditions employed.[14,15] As illustrated in Figure 3, k_{obs} approaches saturation with increasing pH, and A_0^{CALC} and k_{obs} are proportional to one another. The curves can be fit with the following functions both at high and low $[(SCN)_2]_{T,0}$:

$$k_{obs} = \frac{\xi_{12}[OH^-]}{1 + \xi_{13}[OH^-]} \qquad (14)$$

$$k_{obs} = \xi_{14}A_0^{CALC} + \xi_{15} \qquad (15)$$

where ξ_{12}, ξ_{13}, ξ_{14}, and ξ_{15} are pH-independent constants (Table S2), although dependent on $[(SCN)_2]_{T,0}$. The rate law at high $[(SCN)_2]_{T,0}$ is the following:

$$v = \frac{\xi_{16}[OH^-]}{1 + \xi_{17}[SCN^-] + \xi_{18}[OH^-]}[(SCN)_2]_T \qquad (16)$$

where ξ_{16}, ξ_{17}, and ξ_{18} are constants (Table S2) and $[(SCN)_2]_T$ is the time-dependent analytical concentration of $(SCN)_2 + (SCN)_3^-$.

Quenching the decomposition of $(SCN)_2$ with $HClO_4$ in triple-mixing experiments yielded $(SCN)_2$ and quenching with
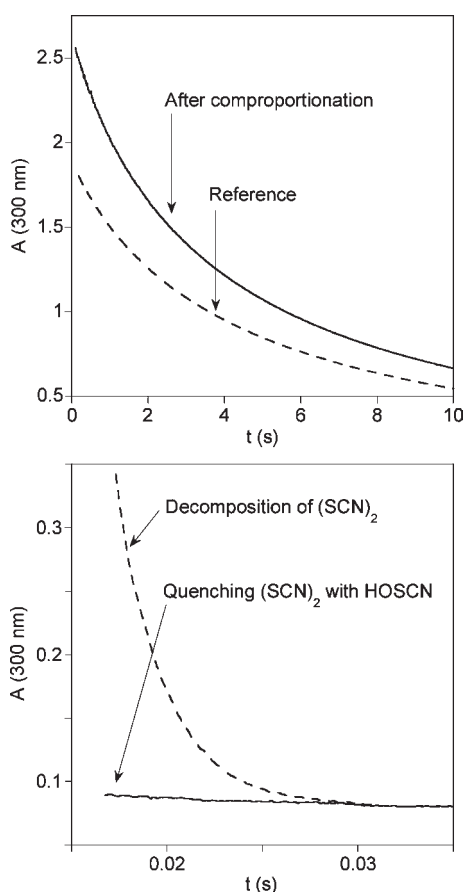
Figure 4. Change in absorbance at 300 nm after directly mixing solutions of $(SCN)_2$ and HOSCN/OSCN$^-$ at pH = 0.70 (top) and at pH = 3.89 (bottom). At pH = 0.70, HOSCN comproportionates with SCN$^-$ to give $(SCN)_2$ which decomposes in a homogeneous second-order reaction. $[(SCN)_2]_{T,0}$ = 1.4 mM, $[HOSCN]_{T,0}$ = 1.1 mM, $[SCN^-]$ = 0.25 M,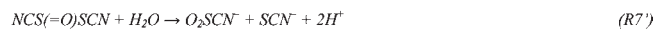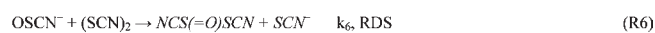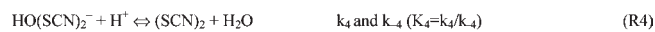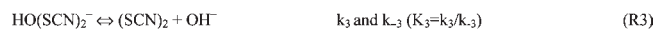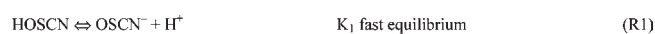 $[HClO_4]$ = 0.20 M, μ = 1.0 M, and 25.0 °C: (dashed line) reference ($[HOSCN]_{T,0}$ = 0); (continuous line) experiment. At pH = 3.89, HOSCN/OSCN$^-$ quenches $(SCN)_2$. $[(SCN)_2]_{T,0}$ = 1.4 mM, $[HOSCN]_{T,0}$ = 1.2 mM, $[SCN^-]$ = 0.25 M, $[HOAc]$ + $[OAc^-]$ = 0.50 M, μ = 1.0 M, and 25.0 °C: (dashed line) reference ($[HOSCN]_{T,0}$ = 0); (continuous line) experiment.

NaOH yielded OSCN$^-$,[18,34] as evident by in situ photometric detection. A significantly larger molar amount of $(SCN)_2$ was produced in the acidic quench than OSCN$^-$ was produced in the basic, and slightly more than the remaining amount of $(SCN)_2$ (vide infra). The data sets were measured with high relative error due to the low absorbance values or insufficient stability of the OSCN$^-$ solutions (Figure S11 of the Supporting Information).

ESI-MS data evidence that CN$^-$, OCN$^-$, SO$_4^{2-}$, and SO$_3^{2-}$ are produced during the decomposition of $(SCN)_2$ at pH 4 (Table 1). No intermediates were identified in the quench-flow/ESI-MS experiments. An excess of SCN$^-$ present in the solutions during the decomposition has no observable effect on the relative amounts of products.

Decomposition of $(SCN)_2$ around pH 7. No kinetic information could be obtained for the decomposition of $(SCN)_2$ since the reaction is complete in the mixing time of the stopped-flow instruments. Thus, on the basis of UV−vis and MS measurements, OSCN$^-$ is excluded as the product of the hydrolysis of

Scheme 1. Mechanism of Decomposition of HOSCN/OSCN$^-$ in the Range from pH 4 to pH 7[a]

HOSCN ⇔ OSCN$^-$ + H$^+$	K$_1$ fast equilibrium	(R1)
HOSCN + SCN$^-$ ⇔ HO(SCN)$_2^-$	k$_2$ and k$_{-2}$ (K$_2$=k$_2$/k$_{-2}$)	(R2)
HO(SCN)$_2^-$ ⇔ (SCN)$_2$ + OH$^-$	k$_3$ and k$_{-3}$ (K$_3$=k$_3$/k$_{-3}$)	(R3)
HO(SCN)$_2^-$ + H$^+$ ⇔ (SCN)$_2$ + H$_2$O	k$_4$ and k$_{-4}$ (K$_4$=k$_4$/k$_{-4}$)	(R4)
(SCN)$_2$ + SCN$^-$ ⇔ (SCN)$_3^-$	K$_5$ fast equilibrium	(R5)
OSCN$^-$ + (SCN)$_2$ → NCS(=O)SCN + SCN$^-$	k$_6$, RDS	(R6)
NCS(=O)SCN + H$_2$O → O$_2$SCN$^-$ + SCN$^-$ + 2H$^+$		(R7')
O$_2$SCN$^-$ + HOSCN → O$_3$SCN$^-$ + SCN$^-$ + H$^+$		(R8')
O$_3$SCN$^-$ + H$_2$O → SO$_4^{2-}$ + HCN + H$^+$		(R9')
O$_3$SCN$^-$ + H$_2$O → SO$_3^{2-}$ + OCN$^-$ + 2H$^+$		(R10')

$$3HOSCN + H_2O \rightarrow XSO_4^{2-} + XHCN + (1\text{-}X)SO_3^{2-} + (1\text{-}X)OCN^- + 2SCN^- + (5\text{-}X)H^+ \quad (R11)$$
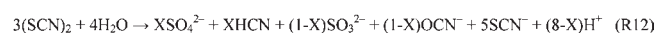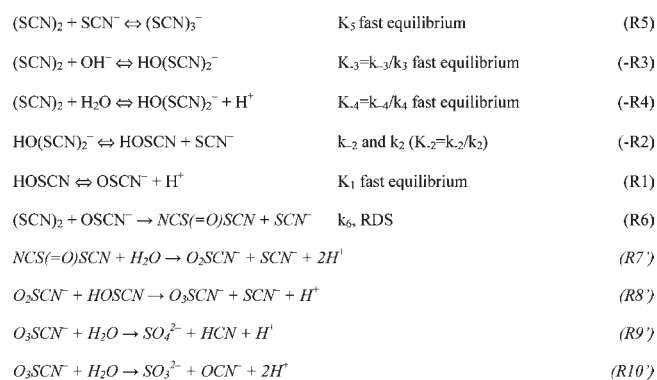
[a] Above the line, proposed kinetic model; below the line, proposed stoichiometry with $X \leq 1$ (k_{-2}, k_{-3}, and k_{-4} are the rate constants of the backward reactions of R2, R3, and R4, respectively; italicized reactions occur after the rate-determining R6 step).

$(SCN)_2$ at pH 7. The eventual products at pH 7 (OCN$^-$, SCN$^-$, SO$_3^{2-}$, and SO$_4^{2-}$) were identified by MS and quantified by IC (the results are given in Table 1).

Reaction of $(SCN)_2$ with HOSCN/OSCN$^-$. Figure 4 illustrates representative results for the reaction of $(SCN)_2$ with HOSCN/OSCN$^-$. When mixing the two reactants at pH = 0.70 and high $[SCN^-]$ with $(SCN)_2$ in small excess over HOSCN, an elevation of the absorbance was observed at 300 nm which corresponds to the production of $(SCN)_2$/$(SCN)_3^-$ during the comproportionation of HOSCN and SCN$^-$.[14] The production of $(SCN)_2$ was complete within 100 ms, and it decomposes with homogeneous second-order kinetics.[14,15] When $(SCN)_2$ was mixed with HOSCN/OSCN$^-$ at pH = 3.89 and high $[SCN^-]$, the absorbance decreased at 300, 306, and 376 nm (compared to the references) and the reaction was over within the mixing time. We were not able to study the kinetics of the process in detail to verify the direct reaction of $(SCN)_2$ with HOSCN/OSCN$^-$ at pH 4, as maintaining the reaction conditions for a series of experiments proved to be technically challenging. However, a semiquantitative observation was made that when $[(SCN)_2]_{T,0}$ was varied from 0.1 to 0.4 mM with $[HOSCN]_{T,0}$ = 0.4 mM, the kinetics showed biphasic characteristics (a first step of 1−2 ms half-life and a second step with a 0.4−0.5 s half-life) with a decrease in absorbance at 300 nm where both $(SCN)_2$ and HOSCN absorb (Figure S12 of the Supporting Information). The measured initial absorbance (t = 0.8 ms) at 300 nm increased with increasing $[(SCN)_2]_{T,0}$, and the starting absorbance of the second step (t = 100 ms) decreased with increasing $[(SCN)_2]_{T,0}$ (Figure S13 of the Supporting Information); thus the first step is associated with the reaction of $(SCN)_2$ with HOSCN/OSCN$^-$. The rate of the second step, the decomposition of the excess HOSCN/OSCN$^-$, also increased with increasing $[(SCN)_2]_{T,0}$. IC analysis of the product solutions was not successful because all of the experiments were carried out in the presence of high concentrations of SCN$^-$.

■ DISCUSSION

Mechanism of Decomposition of HOSCN/OSCN$^-$ in the Range from pH 4 to pH 7. The proposed mechanism of

Scheme 2. Mechanism of Decomposition of $(SCN)_2$ at pH 4[a]

$(SCN)_2 + SCN^- \Leftrightarrow (SCN)_3^-$	K_5 fast equilibrium	(R5)
$(SCN)_2 + OH^- \Leftrightarrow HO(SCN)_2^-$	$K_{-3}=k_{-3}/k_3$ fast equilibrium	(-R3)
$(SCN)_2 + H_2O \Leftrightarrow HO(SCN)_2^- + H^+$	$K_{-4}=k_{-4}/k_4$ fast equilibrium	(-R4)
$HO(SCN)_2^- \Leftrightarrow HOSCN + SCN^-$	k_{-2} and k_2 ($K_{-2}=k_{-2}/k_2$)	(-R2)
$HOSCN \Leftrightarrow OSCN^- + H^+$	K_1 fast equilibrium	(R1)
$(SCN)_2 + OSCN^- \rightarrow NCS(=O)SCN + SCN^-$	k_6, RDS	(R6)
$NCS(=O)SCN + H_2O \rightarrow O_2SCN^- + SCN^- + 2H^!$		(R7')
$O_2SCN^- + HOSCN \rightarrow O_3SCN^- + SCN^- + H^+$		(R8')
$O_3SCN^- + H_2O \rightarrow SO_4^{2-} + HCN + H^!$		(R9')
$O_3SCN^- + H_2O \rightarrow SO_3^{2-} + OCN^- + 2H^+$		(R10')

$3(SCN)_2 + 4H_2O \rightarrow XSO_4^{2-} + XHCN + (1-X)SO_3^{2-} + (1-X)OCN^- + 5SCN^- + (8-X)H^+$ (R12)

[a] Above the line, proposed kinetic model; below the line, proposed stoichiometry with $X \leq 1$ (to be consistent with the definitions in Scheme 1, k_{-2}, k_{-3}, and k_{-4} are the forward rate constants and k_3, k_4, and k_2 are the backward rate constants of reactions −R2, −R3, and −R4, respectively).

decomposition of HOSCN/OSCN$^-$ is illustrated in Scheme 1. Because no second-order behavior was observed, the reaction of two HOSCN and/or OSCN$^-$ molecules cannot be a major pathway under the conditions that were employed.[14,15] The reactive species is HOSCN, both at higher and lower pH. We assume the formation of a previously unknown intermediate HO(SCN)$_2^-$ from HOSCN and SCN$^-$ in a reversible step. SCN$^-$ is regarded as a pseudo-halide and $(SCN)_2$ as a pseudo-halogen on the basis of their chemical reactivity.[14,15,33,35−37] The role of I$_2$OH$^-$ in the hydrolysis chemistry of I$_2$ has been previously described in detail.[28−30] Accordingly, we propose the existence of equilibria R2−R4 (Schemes 1 and 2). The dissociation of HO(SCN)$_2^-$ to $(SCN)_2$ (R3) is assumed, which can be proton-catalyzed at lower pH (R4). The general rate law is given by

$$v = k_6[(SCN)_2][OSCN^-] \quad (17)$$

The steady-state approximation is valid for $[HO(SCN)_2^-]$ and $[(SCN)_2]$, because both species are proposed to be produced slowly and consumed rapidly. Furthermore, their concentrations never exceed low μM that would result in a detectable signal as both $(SCN)_3^-$ (R6) and HO(SCN)$_2^-$ (Table 2) have orders-of-magnitude higher molar absorbances than HOSCN/OSCN$^-$:

$$v = \frac{\alpha(1-\alpha)k_2k_6(k_3 + k_4[H^+])[SCN^-][HOSCN]_T^2}{k_{-2}(k_{-3}[OH^-] + k_{-4}) + (1-\alpha)k_6(k_{-2} + k_3 + k_4[H^+])[HOSCN]_T}$$

$$\alpha = \frac{[H^+]}{K_1 + [H^+]} \text{ and } [HOSCN]_T = [HOSCN] + [OSCN^-] \quad (18)$$

Considering that (see the Supporting Information)

$$k_{-2}(K_1 + [H^+])(k_{-3}[OH^-] + k_{-4})$$
$$\ll K_1 k_6(k_{-2} + k_3 + k_4[H^+])[HOSCN]_T \quad (19)$$

leads to the rate law

$$v = \frac{k_2(k_3 + k_4[H^+])[H^+][SCN^-]}{(k_{-2} + k_3 + k_4[H^+])(K_1 + [H^+])}[HOSCN]_T \quad (20)$$

Table 2. Constants Resulting from Global Fit of the Kinetic Data on the Decomposition of $(SCN)_2$ and HOSCN/OSCN$^-$ in the Region from pH 4 to pH 7

constant	value
K_1	$(1.17 \pm 0.4) \times 10^{-5}$ M [a]
k_2	50.0 ± 0.9 M^{-1} s^{-1}
k_{-2}	$(2.07 \pm 0.09) \times 10^3$ s^{-1}
K_2	2.4×10^{-2} M^{-1} [b]
k_3	137 ± 23 s^{-1}
k_{-3} [c]	3.6×10^{11} M^{-1} s^{-1} [b]
K_{-3}	$(2.65 \pm 0.3) \times 10^9$ M^{-1}
k_4	$(1.29 \pm 0.07) \times 10^8$ M^{-1} s^{-1}
k_{-4}	3.4×10^3 s^{-1} [b]
K_{-4}	2.7×10^{-5} M [b]
K_5	0.54 ± 0.1 M^{-1} [a]
k_6	$(4.01 \pm 0.3) \times 10^6$ M^{-1} s^{-1}
$E_7\{HO(SCN)_2^-\}_{300\,nm}$	1.6×10^3 M^{-1} cm^{-1} [b]

[a] May be compared with the values of $K_1 = 1.41 \times 10^{-5}$ M and $K_5 = 0.43$ M^{-1} that have been previously reported.[15,31,33] [b] Deduced from other constants. [c] The value of k_{-3} (italic) is overestimated; the limiting rate of diffusion is ca. 10^{10} M^{-1} s^{-1} in water.

And, at pH 7 we assume that $k_4[H^+] \ll k_3$ and $[H^+] \ll K_1$; therefore:

$$v = \frac{k_2k_3[H^+][SCN^-]}{K_1(k_{-2} + k_3)}[HOSCN]_T \quad (21)$$

The experimentally determined and the deduced limiting rate laws agree both at pH 4 (eq 9 and eq 20, respectively) and at pH 7 (eq 12 and eq 21, respectively). However, the proposed mechanism does not account for the observed intercepts of the k_{obs} vs [SCN$^-$] and k_{obs} vs [H$^+$] curves at pH 7 (Figure S6 and parameter ξ_9 in Table S2), which clearly indicates the presence of an alternative mechanism at pH ≥ 7 and [SCN$^-$]$_0 \leq$ [HOSCN]$_{T,0}$. The disproportionation of HOSCN/OSCN$^-$ in a bimolecular reaction is a feasible explanation.[14,15] However, at pH > 11, OSCN$^-$ is known to hydrolyze to thiocarbamate S-oxide.[38]

A global data fit was performed to validate our kinetic model: the complete experimental kinetic data set ([SCN$^-$] and pH dependence at pH 4 and pH 7) was fit to the proposed model, with k_{obs} and the initial absorbances at 306 and 376 nm defined as dependent parameters, [H$^+$] and [SCN$^-$] defined as independent parameters, and the floating constants were k_2, k_{-2}, k_3, k_4, ξ_9, K_1, and E_1, E_2, E_3, and E_4 (which were defined as the molar absorptivities of HOSCN at 306 and 376 nm and the molar absorptivities of OSCN$^-$ at 306 and 376 nm, respectively). The model provided an excellent fit of the experimental data. The resulting calculated constants are given in Tables 2 and S3.

Mechanism of Decomposition of $(SCN)_2$ at pH 4. Scheme 2 illustrates the proposed mechanism of the decomposition of $(SCN)_2$. The pH dependence of the initial spectrum around pH 4 is the result of the protolytic equilibria −R3 and −R4, which are considered fast under the applied conditions. The equilibria −R3 and −R4 are competitive with the formation of $(SCN)_3^-$ in R5. Because limiting second-order behavior is expected at low [(SCN)$_2$]$_T$, and limiting first-order behavior was observed at high [(SCN)$_2$]$_T$, a reversible first-order step is proposed to precede a second-order step. We suggest that HOSCN/OSCN$^-$

is produced in the dissociation of $HO(SCN)_2^-$ in $-R2$ and that it subsequently reacts with $(SCN)_2$ in the rate-limiting step R6. The protonation state of the reacting species in R6 cannot be determined on the basis of our kinetic experiments as we were unable to measure the pH dependence of the reaction under second-order conditions, and as all measurements were carried out at least 0.3 pH units below the pK_a of HOSCN (K_1). The properties of reaction R6 are discussed in detail later. In deriving the general rate law, equilibrium $-R4$ was omitted because $K_{-4} = K_{-3}K_w$ and because $OSCN^-$ is assumed to react with $(SCN)_2$ (R6; vide infra). Using the steady-state approximation for $[HOSCN]_T$ and starting with eq 17:

$$\nu = (1-\alpha)k_{-2}k_6K_{-3}[OH^-][(SCN)_2]_T^2$$
$$\times \left(\alpha k_2[SCN^-] + \frac{(1-\alpha)k_6[(SCN)_2]_T}{1 + K_{-3}[OH^-] + K_5[SCN^-]} \right)^{-1}$$
$$\times (1 + K_{-3}[OH^-] + K_5[SCN^-])^{-2}$$
$$\alpha = \frac{[H^+]}{K_1 + [H^+]}$$
$$[(SCN)_2]_T = [(SCN)_2] + [(SCN)_3^-] + [OH(SCN)_3^-]$$

$$(22)$$

For high $[(SCN)_2]_T$ (see the Supporting Information)

$$k_2(1 + K_{-3}[OH^-] + K_5[SCN^-])[H^+][SCN^-]$$
$$\ll k_6K_1[(SCN)_2]_T \qquad (23)$$

and the limiting-rate law is

$$\nu = \frac{k_{-2}K_{-3}[OH^-]}{1 + K_{-3}[OH^-] + K_5[SCN^-]}[(SCN)_2]_T \qquad (24)$$

Thus, reaction $-R2$ is rate-limiting when $[(SCN)_2]_T$ is high. The deduced rate law (eq 24) is the same as the experimentally obtained rate law at high $[(SCN)_2]_{T,0}$ (see Results and eq 16). A global data fit was performed: the experimental data set recorded at high $[(SCN)_2]_{T,0}$ was fit to the limiting first-order model with k_{obs} and A_0^{CALC} as dependent parameters and $[SCN^-]$ and $[OH^-]$ as independent parameters. Floating constants were as follows: k_{-2}, K_{-3}, K_5, and E_5, E_6, and E_7 (which are the molar absorbances of $(SCN)_2$, $(SCN)_3^-$, and $HO(SCN)_2^-$, respectively, at 300 nm). The parameter k_6 was approximated by fitting the following equation to the k_{obs} vs $[(SCN)_2]_{T,0}$ curves recorded at different pH values (Figure 2):

$$k_{obs} = (1-\alpha)k_{-2}k_6K_{-3}[OH^-][(SCN)_2]_{T,0}$$
$$\times \left(\alpha k_2[SCN^-] + \frac{(1-\alpha)k_6[(SCN)_2]_{T,0}}{1 + K_{-3}[OH^-] + K_5[SCN^-]} \right)^{-1}$$
$$\times (1 + K_{-3}[OH^-] + K_5[SCN^-])^{-2}$$
$$\alpha = \frac{[H^+]}{K_1 + [H^+]}$$

$$(25)$$

The experimental data set fits well to the proposed kinetic model, and the obtained constants are listed in Tables 2 and S3.

In spite of the high quality of the fit, the limiting rate laws and therefore the obtained parameters can be regarded only as approximations as seen for example in the value of k_{-3} which exceeds 10^{10} M^{-1} s^{-1}. Although taking into consideration that
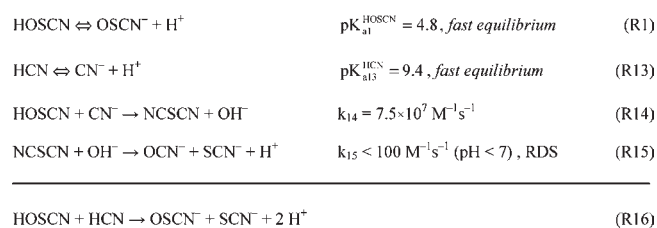
numerous independently recorded data sets were analyzed simultaneously without considering the error of the independent parameters (i.e., initial concentrations and pH), the results are satisfactory.

Reaction of $(SCN)_2$ with HOSCN and/or $OSCN^-$. The hydrolysis of $(SCN)_2$ to $HOSCN/OSCN^-$ is well-defined at both high and at low pH, but not at pH 4–8 because $(SCN)_2$ does not hydrolyze to $HOSCN/OSCN^-$ from pH 4 to 8 (vide supra). Considering the lack of other reactants in the $(SCN)_2$ solution, the simplest explanation for the absence of $HOSCN/OSCN^-$ under the described conditions is that $(SCN)_2$ reacts with $HOSCN/OSCN^-$ faster than $(SCN)_2$ hydrolysis can take place. Indirect evidence was found for the existence of the reaction of $(SCN)_2$ with $HOSCN/OSCN^-$ at pH 4 during the study of the decomposition of $(SCN)_2$ at low $[(SCN)_2]_{T,0}$, and we obtained direct evidence by mixing the two reactants in independent experiments.

The rate-limiting step in the decomposition of HOSCN and $(SCN)_2$ involves the reaction of $OSCN^-$ with $(SCN)_2$ (R6). In principle, the product of such a reaction could be an oxo derivative of the previously characterized $(SCN)_3^-$. However, we have not found a stable ground-state structure for a molecule formulated as $O(SCN)_3^-$ using computational methods (Supporting Information). Accordingly, we have described the reaction of $OSCN^-$ with $(SCN)_2$ (R6) as a substitution to give "$O(SCN)_2$" and SCN^-. The reaction is assumed to take place as a formal SCN^- for $OSCN^-$ substitution because $OSCN^-$ is not known to react as a direct O-donor.[21,31,39] There are two reasonable ground-state structures for "$O(SCN)_2$": NCS−O−SCN (cf. a thiolsulfinate) and NCS(=O)−SCN (cf. a thiosulfenate ester). Remarkably, ab initio quantum chemical calculations yield stable ground states for both structures with very similar total energies (Table S4 of the Supporting Information). However, the activation barriers at room temperature (58 kcal/mol using a MP2/6-311+G** basis set, Figure S14 of the Supporting Information) appears to preclude their interconversion, especially in the time frame of their expected lifetimes. While the calculations do not distinguish between the possible structures, evidence for an asymmetrical intermediate has been previously provided by radio-labeling studies which demonstrated that SO_4^{2-} in a pH 7 solution of $OSCN^-$ and SCN^- is derived exclusively from $OSCN^-$,[19] indicating the conservation of the O−S bond. We therefore propose the intermediate is NCS(=O)SCN.

We were not able to experimentally determine the protonation state of the reactants in R6; and although both HOSCN and $OSCN^-$ could act as nucleophiles toward $(SCN)_2$, the latter is presumably a much better nucleophile. It is improbable that only the $OSCN^-$ is reactive toward $(SCN)_2$, and we exclude this possibility for the explanation of the absence of reaction R6 at pH 0.7. Instead, we propose that R6 becomes reversible, with $(SCN)_2$ as the favored product at low pH. This proposal is supported by the observations made during the triple-mixing quenching experiments. Elevated concentrations of $(SCN)_2$ were observed after the acidic quench of the decomposition of $(SCN)_2$ at pH 4 (Figure S11), which can be accounted for by the conversion of the steady-state intermediates $HOSCN/OSCN^-$ and NCS(=O)SCN to $(SCN)_2$ at low pH. We assume that the excess amount of $OSCN^-$ after the basic quench was slightly less than the excess amount of $(SCN)_2$ after the acidic quench, because NCS(=O)SCN reacts to eventually give SO_4^{2-} and CN^- (reactions R7′−R10′) in the highly basic solution.

Scheme 3. Mechanism of the Reaction of HOSCN with HCN below pH 7

$$HOSCN \leftrightarrow OSCN^- + H^+ \qquad pK_{a1}^{HOSCN} = 4.8, \text{ fast equilibrium} \qquad (R1)$$

$$HCN \leftrightarrow CN^- + H^+ \qquad pK_{a13}^{HCN} = 9.4, \text{ fast equilibrium} \qquad (R13)$$

$$HOSCN + CN^- \rightarrow NCSCN + OH^- \qquad k_{14} = 7.5 \times 10^7 \text{ M}^{-1}\text{s}^{-1} \qquad (R14)$$

$$NCSCN + OH^- \rightarrow OCN^- + SCN^- + H^+ \qquad k_{15} < 100 \text{ M}^{-1}\text{s}^{-1} \text{ (pH < 7), RDS} \qquad (R15)$$

$$HOSCN + HCN \rightarrow OSCN^- + SCN^- + 2 H^+ \qquad (R16)$$

The production of $(SCN)_2$ from HOSCN/OSCN$^-$ is slower by 2 orders of magnitude compared to the production of HOSCN/OSCN$^-$ from $(SCN)_2$; thus, the steady-state concentrations of NCS(=O)SCN and $(SCN)_2$ are practically zero during the decomposition of HOSCN/OSCN$^-$ in the region from pH 4 to pH 7. We note these measurements were only semiquantitative and obtained with large experimental error.

Stability of the Intermediates. HO$(SCN)_2^-$ was not observed during the previous investigations of the hydrolysis of $(SCN)_2$, and the comproportionation of HOSCN and SCN$^-$ in the range from pH 0 to pH 2,[14,15] because HO$(SCN)_2^-$ cannot exist at pH < 3 as $K_{-4} = 2.65 \times 10^{-5}$ ($pK_a^{(SCN)_2} = 4.58$). The intermediate HO$(SCN)_2^-$ can only be a minor transient species in the hydrolysis of $(SCN)_2$ to give OSCN$^-$ at pH > 8 because $-R3$ is a fast equilibrium, and $-R2$ is shifted to the left with the deprotonation of HOSCN.

We propose that NCS(=O)SCN is formed over a wide range of pH (0–8) where $(SCN)_2$ and HOSCN or OSCN$^-$ coexist for some milliseconds, long enough for their reaction. However at high [H$^+$] and [SCN$^-$], reaction R6 becomes reversible and shifts toward the initial compounds. At lower [H$^+$], the rapid hydrolysis of NCS(=O)SCN is assumed. At high [OH$^-$], $(SCN)_2$ is quantitatively converted to HO$(SCN)_2^-$. Thus, the relative rate of formation of NCS(=O)SCN becomes negligible compared to the relative rate of formation of OSCN$^-$. On the basis of these considerations, no intermediates are expected to be detectable with quench-flow/ESI-MS experiments, and none were found.

Fast Steps and Stoichiometry. The proposed mechanism for the hydrolysis of NCS(=O)SCN as seen in Schemes 1 and 2 (R7′–R10′) is based on analogy with the halogens,[35–37] as no kinetic data are available for these fast reactions that take place after the rate-limiting steps. The product ratios determined by the IC experiments (Table 1) differ significantly from the predicted stoichiometry of the reactions as seen in Schemes 1 and 2. We propose that as [CN$^-$] increases during decomposition, its reaction with HOSCN becomes competitive among the fast reactions (Scheme 3, R14 and R15). Reaction R14 has been studied in detail,[21] and its pH-dependent rate is maximal around pH 7, which is in agreement with the observed increase in the OCN$^-$ ratio. Table 1 also contains calculated product ratios indicating the contribution of R16 to the overall decomposition of $(SCN)_2$ and HOSCN/OSCN$^-$. At pH 7, the SCN$^-$ concentration is smaller and the OCN$^-$ concentration is larger than anticipated, which is evidence for an alternative hydrolysis pathway under these conditions. The stoichiometry of the reactions at pH 7 is balanced with inclusion of the production of elementary sulfur (which was detected by ESI-MS); however, the mechanism of its formation is not clear.

Biologically Relevant Reactions. Several important conclusions can be drawn with respect to the biological relevance of the results described herein. First, it is difficult to imagine $(SCN)_2$ playing a significant role as a biological reactive intermediate at neutral pH in an aqueous environment. The usual pathway to produce $(SCN)_2$, comproportionation of HOSCN and SCN$^-$, is magnitudes slower[14] than the reaction of $(SCN)_2$ with OSCN$^-$. Thus, as soon as $(SCN)_2$ is formed, it is already consumed through its reaction with OSCN$^-$, which is a process that also depletes the concentration of OSCN$^-$. Furthermore, if other pathways exist for producing $(SCN)_2$, it is unlikely that $(SCN)_2$ plays a role in aqueous environments where the concentration of OSCN$^-$ is significant (as a consequence of the facile reaction R6), especially in the mucosae where the steady-state concentration of OSCN$^-$ can achieve high micromolar concentrations. Second, we have shown that no mechanistic proposals which involve $(SCN)_2$ as a precursor can be feasible for the formation of OSCN$^-$ at neutral pH[18,19,40–44] because these species are not in dynamic equilibrium. Furthermore, OSCN$^-$ and $(SCN)_2$ cannot coexist longer than a few milliseconds at neutral pH. Third, on the basis of the kinetic data, we have confirmed that relatively short-lived derivatives of OSCN$^-$ are produced during the decomposition of OSCN$^-$, including the product of the reaction of $(SCN)_2$ and OSCN$^-$, which we have formulated as NCS-(=O)SCN on the basis of the results of ab initio MO calculations and isotope tracer studies that favor an unsymmetrical intermediate (vide supra).[19] It is unlikely that the intermediate contains a symmetrical -S–O–S- linkage, as has been suggested in some early literature in the field.[45] Fourth, we found that a high relative concentration of OCN$^-$ is produced during the decomposition of OSCN$^-$ at neutral pH. This raises the question of whether the observed MPO-catalyzed carbamylation of proteins in sites of inflammation is caused by OCN$^-$ as a direct product of the enzymatic oxidation of SCN$^-$, or whether the OCN$^-$ concentration is elevated because of the decomposition of the excess OSCN$^-$ present.[46]

■ CONCLUSIONS

The mechanism of decomposition of the human defense factor HOSCN is a complicated multistepped process near physiological pH. The lifetime of HOSCN decreases with decreasing pH and with increasing SCN$^-$ concentration. Furthermore the presence of $(SCN)_2$ dramatically decreases the availability of HOSCN as a consequence of their rapid reaction with one another.

Some intermediates of the decomposition of HOSCN have already been described in the literature (e.g., $(SCN)_2$ and $(SCN)_3^-$), and some intermediates are proposed exclusively on the basis of the analogy of the pseudo-halide SCN$^-$ with the halides (e.g., HO$(SCN)_2^-$, O$_2$SCN$^-$, O$_3$SCN$^-$); the formation of NCS(=O)SCN in the reaction of $(SCN)_2$ with OSCN$^-$ is proposed for the first time in this study on the basis of modeling of the kinetics (from which the stoichiometry is obtained), ab initio molecular orbital calculations (Supporting Information), and previously published isotope tracer studies[19] (that indicate the intermediate is unsymmetrical). The eventual stable products of the decomposition of HOSCN at neutral pH are mainly simple inorganic anions (e.g., OCN$^-$, SCN$^-$, SO$_3^{2-}$, and SO$_4^{2-}$), some of which can participate further in biochemical reactions.

Several processes described in the present study are highly relevant in a biological setting. Evidence is provided that HOSCN

19918

dx.doi.org/10.1021/ja2083152 |J. Am. Chem. Soc. 2011, 133, 19911–19921

cannot coexist with $(SCN)_2$ at physiological pH and that they are not in dynamic equilibrium with each other. Furthermore, previous mechanistic proposals for the formation of HOSCN in peroxidase systems that invoke $(SCN)_2$ as an intermediate during the enzymatic oxidation of SCN^- with H_2O_2 cannot be correct, because the product of the hydrolysis of $(SCN)_2$ at neutral pH is not HOSCN. On the basis of these conclusions, the biochemical role of $(SCN)_2$ is questionable. However, the possible roles of the other reactive sulfur species that are produced during the decomposition of HOSCN remain to be investigated.

■ EXPERIMENTAL METHODS

Chemicals and Solutions. ACS reagent grade or better chemicals were used without further purification. Ion exchanged and Millipore ultrafiltered (Milli-Q synthesis A10) water was used to prepare all solutions. NaOH solutions were standardized with potassium hydrogen phthalate, and $HClO_4$ solutions with the standardized NaOH solutions. Acetate buffers (pH = 3.7−5.7) were made from NaOAc and $HClO_4$ and phosphate buffers (pH = 5.8−7.8) from KH_2PO_4 and NaOH. The ionic strengths of the solutions were established using $NaClO_4$. NaSCN, NaOAc, KH_2PO_4, and $NaClO_4$ stock solutions contained 1 mM sodium ethylenediamine tetraacetic acid (Na_2EDTA) to mask trace metal impurities. An Orion Sure-Flow Ross combined-pH electrode attached to an Orion expandable ion analyzer E920 was employed for all pH measurements and an Irving-factor correction was applied.[47] The electrode was calibrated following IUPAC recommendations.[48] For UV−vis absorbance measurements an HP8452A diode array photometer was used with a cell with either a 1.0, 5.0, or 10.0 cm path length.

Preparation of NaOCl, $(SCN)_2$, and NaOSCN Solutions. NaOCl stock solutions were prepared by sparging Cl_2 gas (99.5+%) into a 0.3 M solution of NaOH. The process was stopped at a NaOCl concentration less than 0.10 M. The basic NaOCl solutions were standardized by UV−vis spectroscopy[49] and iodometric titration.[50]

For stopped flow measurements, $(SCN)_2$ solutions were generated in situ in the first mixing cycle of the stopped-flow equipment by mixing an acidic (0.2−0.4 M $HClO_4$) solution of NaSCN (0.2−1.2 M) with a slightly acidified (pH = 5−6) solution of HOCl (0.5−10 mM).[14,15] The reactions were complete within the mixing time. At least a 25-fold excess of NaSCN had to be used to avoid the overoxidation of $(SCN)_2$ by HOCl and get quantitative yields of $(SCN)_2$. The highest concentration of $(SCN)_2$ obtained by this method was 5 mM which decomposed with a half-life of some seconds. The analytical concentration of $(SCN)_2$ was determined photometrically, taking into account the formation of $(SCN)_3^-$ in the presence of SCN^-.[33] For analytical measurements, to avoid the high SCN^- background in the samples, $(SCN)_2$ was synthesized in CCl_4 by oxidizing $Pb(SCN)_2$ with Br_2[34,51,52] and was sequentially extracted into a 0.1 M solution of NaOH. $(SCN)_2$ in CCl_4 was standardized photometrically.[34,52]

Solutions of NaOSCN were prepared using three different methods: (1) NaOSCN solutions were generated in situ for stopped-flow measurements in the first mixing cycle of the instruments by mixing a solution of 0.2−1.5 M NaSCN in 0.2−0.4 M NaOH with a solution of 0.5−15 mM NaOCl from pH 11 to pH 12.[32,34,38] The reaction was complete within 2 s, and at least a 50-fold excess of NaSCN was required for a quantitative yield of $OSCN^-$. The maximum concentration of NaOSCN obtained was 7 mM, which was stable for several minutes.[38] (2) Solutions of NaOSCN were generated at pH 7 using the lactoperoxidase system ($LPO/NaSCN/H_2O_2$)[34,40] when the presence of a high excess of SCN^- was undesirable. For quantitative yield, a 4-fold excess of SCN^- over H_2O_2 was required. The maximum concentration of $OSCN^-$ obtained by this method was 4 mM.[34,40] The enzyme was not removed from the system before further experiments. (3) Solutions with 1:1 SCN^- to $OSCN^-$ ratio were prepared by extracting $(SCN)_2$ in

CCl_4 into a solution of 0.1 M NaOH, where $(SCN)_2$ promptly hydrolyzes to $OSCN^-$ and SCN^-.[34,40] Quantitative 1:1 mixtures were obtained when the resulting $OSCN^-$ concentration of the aqueous solutions did not exceed 4 mM. NaOSCN solutions were standardized photometrically.[32,34,38]

General Stopped-Flow and Quenched-Flow Methods. Double-mixing stopped-flow experiments were performed using a Hi-Tech SF-61 DX2 instrument equipped with both a photomultiplier tube (PMT) for single-wavelength detection and a diode array for multiple wavelength detection. A reference PMT is employed in this instrument. Absorbance traces were collected using a Xe arc lamp and an optical cell with a 1.00 cm path length. Triple-mixing stopped-flow and quenched-flow experiments were carried out using a Bio-Logic SFM-400 instrument. A single PMT, a Xe arc lamp, and a 1.00 cm flow-through optical cell were used for absorbance measurement in stopped-flow mode. The instrument can be converted for sample collection in quench-flow mode. The dead time of both stopped-flow instruments were measured by the reaction of 2,6-dichlorophenol−indophenol (DCIP) with ascorbic acid (AA) under pseudo-first-order conditions with AA in excess.[53] By plotting the experimentally obtained k_{obs} values against $[AA]$, deviation from linearity was observed above $k_{obs} = 600 \text{ s}^{-1}$ for the Hi-Tech instrument, which means that higher k_{obs} values can be determined only with the elevation of relative error (see details in the Supporting Information). The dead time of the Hi-Tech instrument is 1.35(3) ms in double-mixing mode. For the Bio-Logic instrument in stopped-flow mode, dead-time calibration was performed whenever switching to a new mixing sequence. Calibration of the aging time was also necessary for the Bio-Logic instrument in triple-mixing stopped-flow and quench-flow mode for every mixing sequence and was carried out according to the recommendation of the manufacturer using the OH^- catalyzed hydrolysis of 2,4-dinitrophenyl acetate. The experimentally determined and the precalculated dead times and aging times were in excellent agreement within 9% RSD. The temperature during all the stopped-flow and quenched-flow measurements was maintained at 25.0 ± 0.1 °C using Lauda RC-20 circulators equipped with chilled water heat exchangers.

Double Mixing Stopped-Flow Measurements (Hi-Tech). To study the kinetics of the decomposition of $(SCN)_2$ or HOSCN/ $OSCN^-$ at a given pH, the in situ generated acidic or basic reagent solution was mixed with the appropriate buffer in the second mixing cycle, and the reaction was followed photometrically. The concentration of the buffer was chosen to be at least in a 100-fold excess over the reactant. The resulting pH was always measured independently. SCN^- was used in high excess and for concentration dependence studies; its concentration was varied in the NaSCN solution used for the generation of the reagents. A 2.0 s aging time before the second mixing (τ_1) gave the highest yield from the in situ prepared reagents and ensured the excellent reproducibility of the experiments. The reaction of $(SCN)_2$ with HOSCN/$OSCN^-$ at pH 1 and pH 4 was also studied by double-mixing stopped-flow. The in situ-generated $(SCN)_2$ (pH 0) was reacted with freshly prepared solutions of NaOSCN (pH 13) to produce a reaction mixture with a pH between 0.58 and 0.70. For experiments around pH 4, the solution of NaOSCN was prepared with a sufficient amount of NaOAc for the resulting mixture to be buffered. NaOSCN was synthesized either by the extraction method or by mixing NaSCN and NaOCl solutions with a hand mixer. The NaOSCN solutions were used within 2 min after synthesis, and a fresh solution was prepared for each experiment. Reference experiments were done without using hypochlorite or $(SCN)_2$ in CCl_4 during the preparation of one or the other reactant.

Triple-Mixing Stopped-Flow and Quench-Flow Measurements (Bio-Logic). Triple-mixing experiments were performed to quench the decomposition of the studied sulfur species and to create an opportunity for quantitative analysis of the reaction mixtures. $(SCN)_2$ or $OSCN^-$ was generated in situ and allowed to decompose at the desired

pH (after mixing with a buffer) for τ_2 aging times; the reaction was quenched either with $HClO_4$ (jump to pH 0) or with NaOH (jump to pH 13). The samples were analyzed either in situ by UV–vis (stopped-flow mode) or externally (quench-flow mode). Reference experiments were performed in double-mixing mode with in situ UV–vis detection.

Electrospray Ionization Mass Spectrometry. ESI-MS measurements were performed with an Agilent 6538 UHD Accurate-Mass Q-TOF MS with a dual ESI ion source. A 5 μL aliquot of each sample solution was introduced via loop injection with a 0.2 mL/min methanol stream. The temperature of the drying gas was 180 °C. The voltage applied on the ion source was 5000 V. Spectra were recorded at 2 GHz and averaged by Masshunter B.03.01 software from Agilent. The m/z scale was calibrated externally using Agilent ESI tune mix (6 points) and corrected internally with Agilent ESI reference mass solution (2 points). The error of the m/z measurement was less than 7.0 ppm in positive mode and less than 6.0 ppm in negative mode. The aim of the MS experiments was to identify the intermediates and products of the decomposition of $(SCN)_2$ and $HOSCN/OSCN^-$ in various pH values. For product identification $(SCN)_2$ and $OSCN^-$ solutions were generated in situ in the Bio-Logic instrument, and after mixing with the appropriate buffer they were collected in quenched-flow mode and allowed to decompose for 5 min. Intermediate identification was achieved using triple-mixing quench-flow experiments (acidic and basic) that were performed with aging times $\tau_2 = 0.5t_{1/2}$, $1t_{1/2}$, and $2t_{1/2}$, which allowed the construction of reaction-time-resolved MS spectra. Approximately 5 min elapsed between sample preparation and the measurements. All samples were diluted 1/10–1/50 before introduction to the MS, to avoid complication from the high ionic strength. All samples were analyzed both in negative and positive ion mode. The process of compound identification and more details on the measurements can be found in the Supporting Information.

Ion Chromatography. Ion chromatography (IC) was performed on a Dionex ICS-3000 instrument. The sample holder tray, column, detector, and cell were thermostatted to 20, 25, 30, and 35 °C, respectively. The injection loop was 10 μL. CN^- and SCN^- were measured using integrated amperometry detection, and OCN^-, SO_3^{2-}, and SO_4^{2-} were measured using conductivity detection. An Ionpac AS16 column was used for the anions measured, using integrated amperometry detection, and the eluents were as follows: from -5 (preinjection equilibrium) to $+10$ min, isocratic 6.25 mM NaOH; from 10 to 25 min, isocratic 60 mM NaOH. An Ionpac AS18 column and an ASRS 2 mm suppressor were used for ions detected by conductivity, and isocratic 12.5 mM NaOH was employed for 30 min. Each sample was injected three times to ensure reproducibility. Calibration of the methods was performed using a series of standard solutions. The IC measurements were performed to quantify the anions produced during the decomposition of the investigated sulfur species at different pH values. Because SCN^- is one of the expected products, synthetic methods which require an initial large excess of SCN^- were not feasible for these experiments. $(SCN)_2$ was synthesized in CCl_4 and extracted directly to a 50 mM acetate or phosphate buffer, to a concentration of less than 5 mM $(SCN)_2$ in the aqueous phase and was allowed to decompose for 15 min before the analysis. $OSCN^-$ was produced by extracting $(SCN)_2$ synthesized in CCl_4 to a 0.1 M NaOH solution, which was immediately mixed with a phosphate or acetate buffer during constant stirring. $OSCN^-$ was alternatively prepared by using the LPO system in the region from pH 6.5 to pH 7.3 in phosphate buffer. The resulting $HOSCN/OSCN^-$ solutions, regardless of the method of synthesis, contained 50 mM buffer and a maximum of 2 mM reactant. Solutions of $HOSCN/OSCN^-$ were allowed to completely decompose for 30 min prior to analysis. To study the effect of initial SCN^- excess on the decomposition products which was present during all the kinetic studies, additional experiments were performed with buffer solutions containing 8- to 11-fold SCN^- excess over the reactants. All samples were diluted to 10-fold by a NaOH

solution to a final pH of 13 before analysis. Background samples were prepared from the buffers.

Data Treatment. The raw data sets generated in the various types of measurements were treated with the instrument-controlling software. Further manipulation, when necessary, was done by MS Excel 2003 (Microsoft). Specfit/32 (Spectrum Software Associates) was used for the evaluation of polychromatic UV–vis data. Levenberg–Marquard least-squares fits and kinetic data simulations were performed with Scientist 2.0 (Micromath).

■ ASSOCIATED CONTENT

ⓢ Supporting Information. Experimental and computational details, equations used for global fits, schemes showing the Bio-Logic SFM-400 flow chart and stopped-flow parameters of the Hi-Tech SF-61 DX2, figures displaying the concentration and pH dependences of the measured values of k_{obs} during the decomposition of HOSCN and $(SCN)_2$, UV-vis spectra of HOSCN and $OSCN^-$, results of triple-mixing experiments to quench decomposition of $(SCN)_2$, experiments for mixing $(SCN)_2$ with HOSCN, details of the molecular orbital calculations and a reaction coordinate diagram for the interconversion of NCS–O–SCN and NCS(=O)–SCN, a table identifying ESI-MS peaks, a table with the empirical rate constants for the experimentally determined rate laws, a table of computed molar absorptivities obtained from a global fit, and a table of computed total energies for the two ground states and one transition state structures of $O(SCN)_2$. This material is available free of charge via the Internet at http://pubs.acs.org.

■ AUTHOR INFORMATION

Corresponding Author
MAshby@ou.edu

■ ACKNOWLEDGMENT

■ REFERENCES

(1) Ashby, M. T. *J. Dent. Res.* **2008**, *87*, 900.
(2) Hawkins, C. L. *Free Radical Res.* **2009**, *43*, 1147.
(3) Reiter, B.; Harnulv, G. *J. Food Prot.* **1984**, *47*, 724.
(4) Pruitt, K. M.; Tenovuo, J. O., Eds. *The Lactoperoxidase System: Chemistry and Biological Significance*, Immunology Series, Vol. 27; Dekker: New York, 1985.
(5) Ihalin, R.; Loimaranta, V.; Tenovuo, J. *Arch. Biochem. Biophys.* **2006**, *445*, 261.
(6) Pruitt, K. M. *J. Oral Pathol.* **1987**, *16*, 417.
(7) Boots, J. W.; Floris, R. *Int. Dairy J.* **2006**, *16*, 1272.
(8) Seifu, E.; Buys, E. M.; Donkin, E. F. *Trends Food Sci. Technol.* **2005**, *16*, 137.
(9) Pruitt, K. *Advanced Dairy Chemistry*, 3rd ed.; 2003; Vol. 1, p 563.
(10) Naidu, A. S. *Nat. Food Antimicrob. Syst.* **2000**, 103.
(11) Wolfson, L. M.; Sumner, S. S. *J. Food Prot.* **1993**, *56*, 887.
(12) Wang, J.-G.; Mahmud, S. A.; Nguyen, J.; Slungaard, A. *J. Immunol.* **2006**, *177*, 8714.
(13) Wang, J.-G.; Mahmud, S. A.; Thompson, J. A.; Geng, J.-G.; Key, N. S.; Slungaard, A. *Blood* **2006**, *107*, 558.
(14) Nagy, P.; Lemma, K.; Ashby, M. T. *Inorg. Chem.* **2007**, *46*, 285.

(15) Barnett, J. J.; McKee, M. L.; Stanbury, D. M. *Inorg. Chem.* **2004**, *43*, 5021.

(16) Rayson, M. S.; Mackie, J. C.; Kennedy, E. M.; Dlugogorski, B. Z. *Inorg. Chem.* **2011**, *50*, 7440.

(17) Mamman, S.; Iyun, J. F. *Int. J. Pure Appl. Chem.* **2007**, *2*, 429.

(18) Aune, T. M.; Thomas, E. L. *Eur. J. Biochem.* **1977**, *80*, 209.

(19) Thomas, E. L. *Biochemistry* **1981**, *20*, 3273.

(20) Walden, P.; Audrieth, L. F. *Chem. Rev.* **1928**, *5*, 339.

(21) Lemma, K.; Ashby, M. T. *Chem. Res. Toxicol.* **2009**, *22*, 1622.

(22) Kornath, A.; Blecher, O.; Ludwig, R. *J. Am. Chem. Soc.* **1999**, *121*, 4019.

(23) Kornath, A.; Blecher, O. *Z. Anorg. Allg. Chem.* **2002**, *628*, 625.

(24) Jander, G.; Gruttner, B.; Scholz, G. *Chem. Ber.* **1947**, *80*, 279.

(25) Okulik, N. B.; Jubert, A. H.; Castro, E. A. *Adv. Quantum Chem. Bonding Struct.* **2008**, 119.

(26) Okulik, N. B.; Jubert, A. H.; Castro, E. A. *J. Struct. Chem.* **2008**, *49*, 922.

(27) Boehland, H.; Golub, A. M.; Koehler, H.; Lisko, T. P.; Samoilenko, V. M.; Skopenko, V. V.; Cincadze, G. V. *Chemistry of Pseudohalides*; Dr. Alfred Huethig Verlag: Heidelberg, Germany, 1979.

(28) Lengyel, I.; Epstein, I. R.; Kustin, K. *Inorg. Chem.* **1993**, *32*, 5880.

(29) Palmer, D. A.; Van Eldik, R. *Inorg. Chem.* **1986**, *25*, 928.

(30) Truesdale, V. W.; Luther, G. W.; Greenwood, J. E. *Phys. Chem. Chem. Phys.* **2003**, *5*, 3428.

(31) Nagy, P.; Jameson, G. N. L.; Winterbourn, C. C. *Chem. Res. Toxicol.* **2009**, *22*, 1833.

(32) Ashby, M. T.; Carlson, A. C.; Scott, M. J. *J. Am. Chem. Soc.* **2004**, *126*, 15976.

(33) Barnett, J. J.; Stanbury, D. M. *Inorg. Chem.* **2002**, *41*, 164.

(34) Nagy, P.; Alguindigue, S. S.; Ashby, M. T. *Biochemistry* **2006**, *45*, 12610.

(35) Figlar, J. N.; Stanbury, D. M. *J. Phys. Chem. A* **1999**, *103*, 5732.

(36) Figlar, J. N.; Stanbury, D. M. *Inorg. Chem.* **2000**, *39*, 5089.

(37) Nagy, P.; Beal, J. L.; Ashby, M. T. *Chem. Res. Toxicol.* **2006**, *19*, 587.

(38) Nagy, P.; Wang, X.; Lemma, K.; Ashby, M. T. *J. Am. Chem. Soc.* **2007**, *129*, 15756.

(39) Skaff, O.; Pattison, D. I.; Davies, M. J. *Biochem. J.* **2009**, *422*, 111.

(40) Aune, T. M.; Thomas, E. L.; Morrison, M. *Biochemistry* **1977**, *16*, 4611.

(41) van Dalen, C. J.; Whitehouse, M. W.; Winterbourn, C. C.; Kettle, A. J. *Biochem. J.* **1997**, *327*, 487.

(42) Van Dalen, C. J.; Kettle, A. J. *Biochem. J.* **2001**, *358*, 233.

(43) Slungaard, A.; Mahoney, J. R., Jr. *J. Biol. Chem.* **1991**, *266*, 4903.

(44) Das, D.; De, P. K.; Banerjee, R. K. *Biochem. J.* **1995**, *305*, 59.

(45) Pollock, J. R.; Goff, H. M. *Biochim. Biophys. Acta* **1992**, *1159*, 279.

(46) Wang, Z.; Nicholls, S. J.; Rodriguez, E. R.; Kummu, O.; Hörkkö, S.; Barnard, J.; Reynolds, W. F.; Topol, E. J.; DiDonato, J. A.; Hazen, S. L. *Nature Med.* **2007**, *13*, 1176.

(47) Irving, H. M.; Miles, M. G.; Pettit, L. D. *Anal. Chim. Acta* **1967**, *38*, 475.

(48) Covington, A. K.; Bates, R. G.; Durst, R. A. *Pure Appl. Chem.* **1983**, *55*, 1467.

(49) Adam, L. C.; Fabian, I.; Suzuki, K.; Gordon, G. *Inorg. Chem.* **1992**, *31*, 3534.

(50) Gordon, G.; Pacey, G. E.; Cooper, W. J. *Water Chlorination* **1990**, *6*, 29.

(51) Wood, J. L. *Org. React. (New York, NY, United States)* **1946**, 240.

(52) Lemma, K.; Ashby, M. T. *J. Org. Chem.* **2008**, *73*, 3017.

(53) Tonomura, B.; Nakatani, H.; Ohnishi, M.; Yamaguchi-Ito, J.; Hiromi, K. *Anal. Biochem.* **1978**, *84*, 370.